COMPREHENSIVE EVALUATION ON THE THERMAL-HYDRAULIC PERFORMANCE OF SUPERCRITICAL CO_2/R41 IN A MICRO-FIN TUBE

by

Ruoyu DAI, Xixia XU, Yi WANG, Yue WU, and Jieqing ZHENG*

Fujian Province Key Laboratory of Energy Cleaning Utilization and Development, Jimei University, Xiamen, China

Original scientific paper
https://doi.org/10.2298/TSCI220311097D

A 3-D flow and heat transfer theoretical model was established for a 5 mm micro-fin tube to explore the heat transfer and flow characteristics of supercritical CO_2/R41 therein under different pressures, mass fluxes, and components. The research attempts to provide reference for selecting components of working media and setting the pressure and mass flux in different application scenarios. Results show that the closer the temperature of the working medium to the critical temperature, the larger the local convective heat transfer coefficient (CHTC). The CHTC at the critical temperature is 8 to 16 times higher compared with that at the non-critical temperature. The maximum CHTC is greater and the temperature corresponding to the maximum CHTC is lower when the mixed working medium is at a pressure closer to the critical pressure. The maximum CHTC under 7.0 MPa is twice that at 8.0 MPa. As the mass flux increases from 400 to 800 kg/m^{2}s, the CHTC at the non-critical temperature increases by 1.7 times, while the comprehensive evaluation results of heat transfer and pressure drop decrease significantly. When the CO_2 fraction increases from 20.5% to 75%, the maximum CHTC is increased by 2.6 times.

Key words: *supercritical CO_2/R41, micro-fin tube, heat transfer enhancement, drag reduction of flow, numerical simulation*

Introduction

Energy conservation and carbon reduction have become the premise and goal in the development of the whole world. After the use of freon was banned, many types of new refrigerants have flourished. Despite this, there is still a lack of a leading refrigerant. Previously, the commonly used new refrigerants are mainly hydrofluorocarbons, however, their poor flow and heat transfer properties exclude them from being used as perfect substitutes for R22. Supercritical CO_2 is acknowledged as the most promising refrigerant among engineering and academic circles due to its excellent flow and heat transfer properties, GWP as low as 1, and outstanding safety and stability [1]. Therefore, numerous scholars have studied supercritical CO_2 and found that the heat transfer performance of the supercritical working medium is sig-

*Corresponding author, e-mail: zhengjieqing@jmu.edu.cn

nificantly improved at the transcritical state [2]. Hence, the research on supercritical fluids focuses on their flow and heat transfer properties near the critical temperature, however, supercritical working media generally have unstable physical parameters, so that they feature very complex heat transfer properties near the critical temperature. Pioro [3] experimentally classified heat transfer regimes at the transcritical state into normal heat transfer, improved heat transfer, and deteriorated heat transfer according to the influences of thermophysical properties, buoyancy, and acceleration. In addition, two special phenomena, pseudo-boiling [4] and pseudo-film boiling [5], are found likely to occur to heating channels at the critical temperature, which are finally attributed to significant variations of thermophysical properties near the critical and pseudocritical points. Kim and Kim [6] experimentally investigated heat transfer in CO_2 flowing vertically upwards and downwards in a smooth tube under critical conditions. They found that there is a significant peak wall temperature in the vertical upward flow, while there is no such peak temperature in vertical downward flow, due to the relationship between the flow and direction of the buoyancy force. Peng *et al.* [7] explored the heat transfer properties of supercritical CO_2 in micro-channels and found that the heat transfer behaviours differ greatly under the same q/G condition due to the differences in mass flux: there is deteriorated heat transfer when the mass flux is greater than 200 kg/m^{2}s, while no abnormal phenomenon occurs in the case that the mass flux is lower than that value.

Despite the excellent heat transfer properties of supercritical CO_2 at the transcritical state, the high operating pressure and low COP thereof still limit its popularisation and application. Considering this, many scholars have tried to add other materials in supercritical CO_2 to prepare zeotropic refrigerants for improvement [8-14]. Numerous theoretical and experimental studies, Zhang *et al*. [8], Onaka *et al*. [9], Sarkar *et al*. [10], Ali *et al*. [11], and Kim [12, 13], reveal that the mixture of refrigerant R170 or R744 with CO_2 as a heat transfer medium can improve the COP and reduce the operating pressure of a system. Dai *et al*. [14] evaluated the heat transfer properties of ten working media including R41, R161, R134a, and R152a blended with CO_2. They found that CO_2/R41 as a mixed refrigerant shows the optimal performance because of its high COP, low high-side pressure, and the robust performance under the condition of low external temperature glide. Wang *et al*. [15] studied the utilisation effect of CO_2/R41 in a refrigerated cabinet, and found that the use of a CO_2/R41 (51.4/48.6) mixture decreases the optimal peak pressure by 28.62% and at the same time improves the maximum COP by 20.52%, along with an effective reduction of flammability of R41. Compared with pure CO_2, Yu *et al.* [16] found that the COP of a CO_2/R41 blending system exhibits maximum improvements of 14.5% and 25.7% (separately) in heating and cooling mode, respectively. Therefore, supercritical CO_2/R41 has become one of the most attractive coolants due to its leading COP, stability, heat transfer properties, and low working pressure relative to other mixed working media.

Apart from the blending of working media, the design of exchangers also greatly influences the heat transfer and flow properties of a system. At present, research on supercritical CO_2/R41 mainly focuses on its heat transfer properties in small-diameter smooth tubes [12, 13]. In comparison, there is little research on the heat transfer and flow properties of mixed working media in a common type of exchangers such as micro-fin tubes [17], spiral tubes, and tubes arranged in a zig-zag form [18]. Among them, micro-fin tubes have been widely used in devices reliant of refrigerants, including air conditioners, due to their extremely good heat transfer performance, small size, lightness, and reasonable cost. Compared with smooth tubes, the heat transfer enhancement of micro-fin tubes is attributable to the thread structure inside, which significantly enlarges the heat transfer area of the working media and enhances

the turbulence intensity of fluids within [19, 20]. In addition to these, the structure also prevents the fluids from forming a thick boundary-layer, which makes the heat transfer effect of micro-fin tubes be at least 1.8 times higher than smooth tubes [21]. With the development of industries including air conditioners and progress in manufacturing technologies, further challenges have been set for the miniaturised design size and compactness of exchangers [22]. The design size of micro-fin tubes has been reduced from the original 9.52 mm to a later 7 mm, and finally to 5 mm or even smaller. A smaller tube diameter means that an equal volume of working medium has a larger heat transfer area. Besides, a smaller tube diameter also confers higher load-bearing capacity to the micro-fin tubes, which lays a foundation for the use of high-pressure supercritical working media in micro-fin tubes.

At present, there are few references available in the research on the thermo-hydraulic performance of supercritical CO_2/R41 in micro-fin tubes. Moreover, the comprehensive evaluation of the heat transfer enhancement and energy loss of supercritical mixed working media in micro-fin tubes is rarely studied. To address this problem, CFD simulation was used here to conduct in-depth research into the topic, in order to provide theoretical support for the selection of working media for the first time under different working conditions and application scenarios. At first, the heat transfer and flow properties of the supercritical CO_2/R41 in micro-fin tubes were numerically modelled and computed. Then, the CHTC and pressure drop of the mixed working medium with different mixing proportions were compared under different working conditions. Finally, the overall effect was comprehensively evaluated.

Numerical simulation

Geometrical model

In the structural construction of a micro-fin tube, a small-diameter tube must be selected considering the high working pressure and requirements for the huge heat-exchange capacity. By referring to the geometrical structure of a micro-fin tube with an external diameter of 5 mm (as evinced by Ding and Liu [23]), the tube was set to have a length of 400 mm. The structure is illustrated in fig. 1 and the specific parameters are listed in tab. 1.

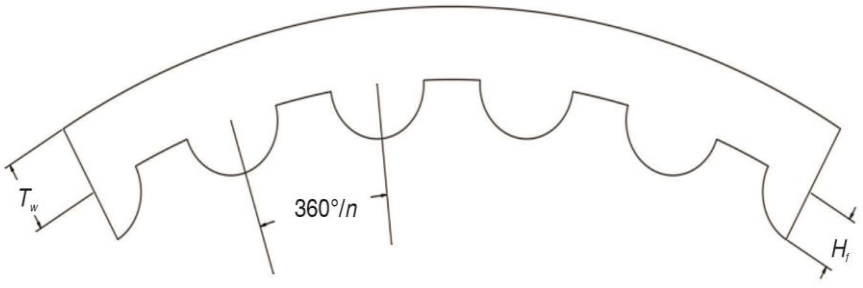

Figure 1. Structure of a micro-fin tube

Table 1. Structural parameters of a micro-fin tube

External diameter, D [mm]	Wall thickness T_w [mm]	Teeth depth, H_f [mm]	Helical angle β [°]	Number of teeth, N
5.00	0.20	0.15	18	30

Governing equations

Currently, there are a variety of simulation methods that can calculate supercritical fluids, such as Reynolds average N-S (RANS), direct numerical simulation (DNS), large eddy simulation (LES), lattice Boltzmann method (LBM), *etc*., among which the first two are the main methods. In principle, DNS can accurately solve all turbulence problems, because it does not contain any artificial assumptions and empirical constants, and its calculation is far more than other methods, which can reduce the calculation cost through the supplement of models [24]. The RANS is slightly less accurate than DNS, but it can solve engineering problems in all Reynolds number range quickly under appropriate application scenarios and stress models [25]. As this numerical simulation is a steady-state simulation of pipeline flow, RANS is selected as the method of this study because it can give consideration to both accuracy of results and cost saving of calculation.

In this paper, RANS *k*-ε turbulence model is used to describe the flow process of the supercritical mixed working medium. The governing equations include the mass conservation equation, momentum conservation equation, energy conservation equation, and relevant equations of the turbulence model follows:

– Mass conservation equation

Conservation of mass means that the mass of a fluid contained in a fluid system remains constant in the course of motion. The differential form of the equation is:

$$\frac{\partial \rho}{\partial t}+\frac{\partial(\rho u)}{\partial x}+\frac{\partial(\rho v)}{\partial y}+\frac{\partial(\rho w)}{\partial z}=0 \tag{1}$$

In steady-state conditions, it is written in the tensor form used by COMSOL:

$$\rho\nabla\cdot\mathbf{u}=0 \tag{2}$$

– Momentum conservation equation

Momentum conservation means that the rate of change in time of momentum in a fluid system is equal to the sum of external forces acting on it. The differential form of the equation is:

$$\rho\frac{D\mathbf{u}}{Dt}=\rho F_b+\frac{\partial p_x}{\partial x}+\frac{\partial p_y}{\partial y}+\frac{\partial p_z}{\partial z} \tag{3}$$

Ignoring gravity, rewrite it as a tensor form containing impulse:

$$\rho(\mathbf{u}\cdot\nabla)\mathbf{u}=\nabla\cdot\left\{-p\mathbf{I}+(\mu+\mu_T)\left[\nabla\mathbf{u}+(\nabla\mathbf{u})^T\right]\right\}+\mathbf{F} \tag{4}$$

– Energy conservation equation

Conservation of energy means that the increase rate of energy in a cell is equal to the net heat flow into the cell plus the work done by the force on the cell. The conservation of energy is expressed as a temperature-dependent equation:

$$\rho C_p\mathbf{u}\cdot\nabla T+\nabla\cdot(-\lambda\nabla T)=Q \tag{5}$$

– RANS *k*-ε turbulence model equations

Turbulent kinetic energy *k* equation is:

$$\rho(\mathbf{u}\cdot\nabla)k=\nabla\cdot\left[\left(\mu+\frac{\mu_T}{\sigma_k}\right)\nabla k\right]+\mu_T\left[\nabla\mathbf{u}:\left(\nabla\mathbf{u}+(\nabla\mathbf{u})^T\right)\right]-\rho\varepsilon \tag{6}$$

Dissipation rate ε equation is:

$$\rho(\mathbf{u}\cdot\nabla)\varepsilon = \nabla\cdot\left[\left(\mu+\frac{\mu_T}{\sigma_\varepsilon}\right)\nabla\varepsilon\right]+C_{\varepsilon 1}\frac{\varepsilon}{k}\mu_T\left[\nabla\mathbf{u}:\left(\nabla\mathbf{u}+(\nabla\mathbf{u})^T\right)\right]-C_{\varepsilon 2}\rho\frac{\varepsilon^2}{k} \tag{7}$$

The calculation formula of eddy viscosity is:

$$\mu_T = \rho C_\mu \frac{k^2}{\varepsilon} \tag{8}$$

Boundary conditions and meshing

The commercially available software COMSOL was used for numerical simulation, in which the flow field and temperature field were calculated in coupling using the Kays-Crawford heat transfer turbulence model. The physical parameters were calculated using the REFPROP9.1 and then imported in the COMSOL to establish a piece-wise cubic interpolation function taking temperature as an independent variable.

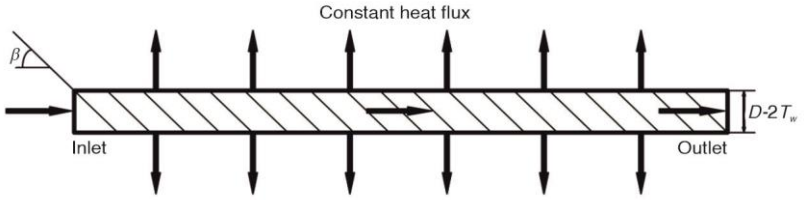

Figure 2. Physical model for the numerical simulation

As for the boundary conditions, the mass flux from 200 to 1000 kg/m^{2}s was set at the inlet;, the temperature at the inlet decreased constantly from 90 ℃ so that the overall temperature in the simulation spanned a range from 20 to 80 ℃, to ensure coverage of the critical temperatures of the mixed working medium under various conditions. Pressures ranging from 7 MPa to 8 MPa were set at the outlet. The constant outward-radiating heat flux of 24 kW/m^2 was set on the wall of the micro-fin tube, as illustrated in fig. 2.

Free tetrahedral elements were used for mesh generation. Elements on the surface of the tube were refined while those at the centre were coarser, allowing modelling of complex flow on the wall and reduction of computational burden. In addition, ten layers of elements were generated for the boundary-layer on the wall to further ensure the accuracy for simulation of the flow. To conduct the mesh-independence test, the number of elements was separately set to 1236884, 920927, 840858, and 686791. Only the size of the grid is changed, but the topology of the grid and the number of boundary-layer grid layers are not changed. Trials were conducted using CO_2/R41 (51.4/48.6) with a mass flux of 400 kg/m^{2}s and pressure of 7.0 MPa, and the CHTC, *h*, was calculated at four temperature points. It can be seen from the fig. 3 that there is no significant difference between the four grids at 33.58 ℃ and 62.535 ℃, which are far away from the critical point. However, at 40.854 ℃ close to the critical point, the CHTC calculated by 686791 and 840858 grids fluctuated greatly. The results of the remaining two grids differ by less than 1% at four temperatures. To improve the calculation accuracy and reduce the computational burden, the number of 920927 was used. The mesh is shown in fig. 4.

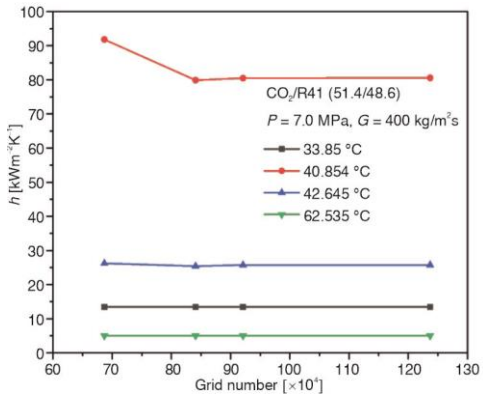

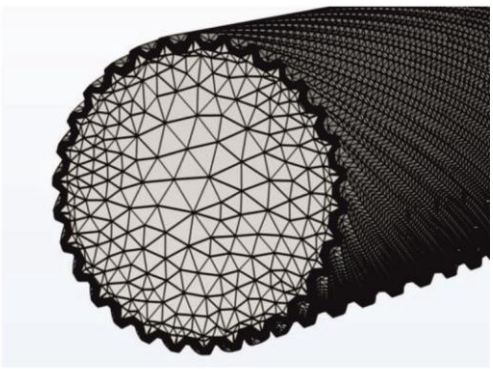

Figure 3. Grid Mesh independence test Figure 4. The finite element mesh structure

Processing of calculation results

The 400 mm long micro-fin tube is divided into five sections, each with a length of 80 mm. The model is divided into multiple sections in order to conveniently remove the inlet section, and multiple sections can be averaged to reduce the error when the CHTC changes slowly, or single section can be selected to prevent the change trend from being blurred when the CHTC changes violently. The inlet temperature $T_{in}(i)$, outlet temperature $T_{out}(i)$, and wall temperature $T_{wall}(i)$ of each section are read using the surface mean function in the analysis of calculation results. The bulk temperature of fluids in the i^{th} section is defined:

$$T_b(i) = \frac{T_{in}(i) + T_{out}(i)}{2}, \quad i = 1,2,3,4,5 \tag{9}$$

Then the CHTC of the i^{th} section is:

$$h(i) = \frac{q}{T_b(i) - T_{wall}(i)} \tag{10}$$

At the boundary-layer of the fluid in the tube, the heat transfer is dominated by heat conduction due to the low convective heat transfer, so the heat transfer capacity is poor there-at. The inlet of the heat-exchange tube is not fully developed, so it is much thinner than the fully developed boundary-layer and its CHTC can be improved. In addition, the inlet shows much greater turbulence energy than other parts, which greatly increases the flow disturbance and further the CHTC. All these make the CHTC at the inlet obviously higher than the normal level. As displayed in fig. 5, the turbulence energy decreases abruptly from the inlet and tends to stabilise at about 70 mm. Therefore, the first section (the first 80 mm along the tube) is eliminated in the data analysis.

The average CHTC is:

$$h = \frac{1}{4}\sum_{i=2}^{5} h(i) \tag{11}$$

After deducting the first section which is not fully developed, the temperature, T_b, of the supercritical fluid in the tube is defined:

$$T_b = \frac{T_{in}(2) + T_{out}(5)}{2} \tag{12}$$

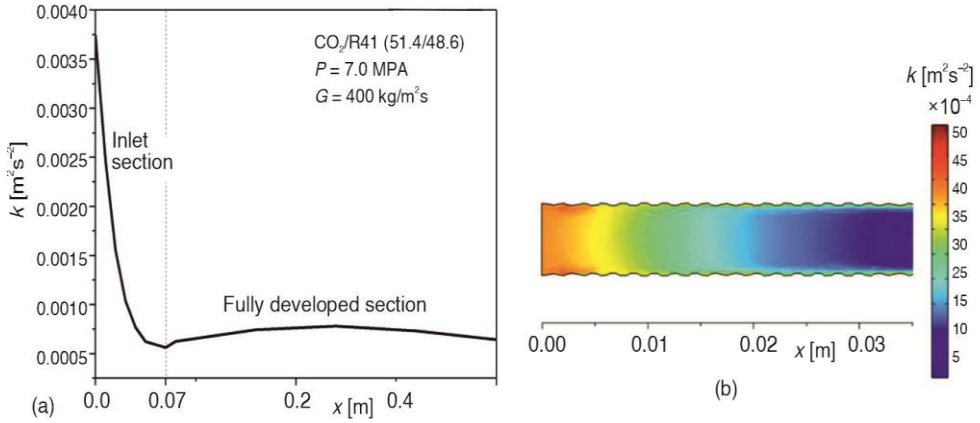

Figure 5. Selection basis for the computation section; (a) distribution of turbulence energy along the length and (b) cloud picture of the local turbulence energy at the inlet section

Eight temperatures are set at the inlet, *i.e.* 90 ℃, 66 ℃, 54 ℃, 48 ℃, 45 ℃, 42 ℃, 39 ℃, and 33 ℃, to calculate the CHTCs of CO_2/R41 in the micro-fin tube at different temperatures: because the performance of the supercritical working medium changes remarkably at the critical temperature, the local CHTC are taken at the critical temperature to avoid data distortion due to reduction of CHTC peaks if taking averages thereof.

The pressure drop is:

$$\Delta p = \frac{p_{\text{in}}(2) - p_{\text{out}}(5)}{2} \tag{13}$$

The purpose of calculating from the second segment is to remove interference from the inlet.

The heat transfer coefficient per unit pressure drop used for comprehensive evaluation is:

$$\alpha = \frac{h}{\mathrm{d}p/\mathrm{d}z} \tag{14}$$

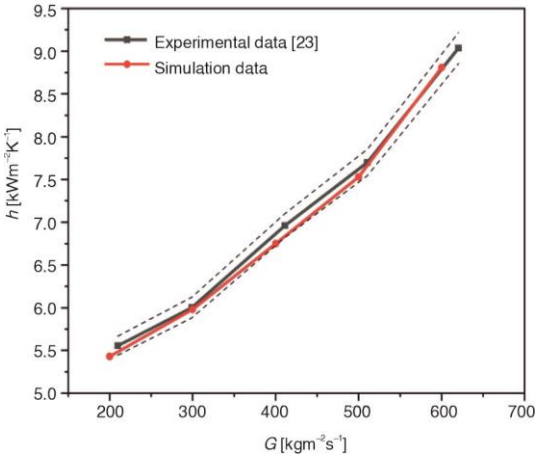

Figure 6. Model validation

Model validation

The previous model was used while the working medium was replaced with R404A. The average CHTC of the medium at different mass fluxes in the micro-fin tube were calculated and then compared with experimental data from previous research under the same working conditions, Ding [23]. Figure 6 shows the changes of the CHTC, *h.* with the mass flex, *G*, in which the dotted lines enclose an error range of within 2%. The maximum deviation between the simulation data and the experimental data is 1.87%, indicative of the reliability of the numerical model.

Results and discussion

Influences of pressure

The pressure affects physical parameters and therefore the heat transfer properties of the mixed working medium in the micro-fin tube. The critical pressures of CO_2 and R41 are 7.39 MPa and 5.90 MPa, respectively. Because of this, the mixed working medium in which R41 accounted for a large proportion was selected to reduce the critical pressure, thus decreasing the requirements imposed on the mixed working medium under the working conditions prevailing in actual applications. According to the REFPROP9.1 data, CO_2/R41 (51.4/48.6) has a critical pressure of 6.8 MPa, so three pressures 7.0 MPa, 7.5 MPa, and 8.0 MPa were used to compare the heat transfer properties.

Figure 7(a) shows changes of the CHTC of the supercritical CO_2/R41 mixture in the micro-fin tube with the temperature and working pressure under a pressure of 7.0 MPa to 8.0 MPa, heat flux of 24 kW/m^2, and mass flux of 400 kg/m^{2}s, respectively. Meanwhile, changes of the CHTC of the mixed working medium in a 2 mm smooth tube measured in the experiment under 7.0 MPa are also illustrated. It can be seen that the CHTC, h, of the CO_2/R41 mixture first increases, then decreases with increasing bulk temperature, T_b, in the micro-fin tube. The CHTC, h, increases abruptly and is maximised near the critical temperature. Besides, the temperature, T_b, corresponding to the maximum CHTC is slightly higher than the critical temperature. This is because the CHTC increases the peak value when the boundary-layer reaches the critical temperature, while the temperature of the boundary-layer is lower than the bulk temperature.

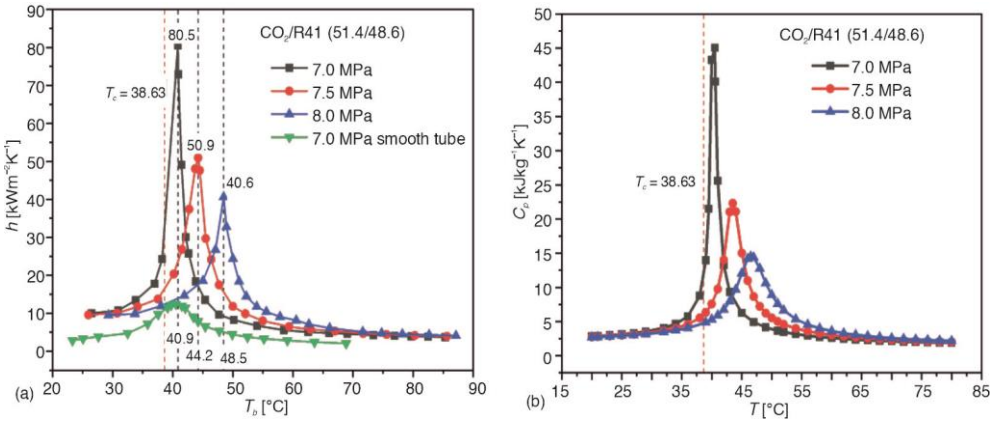

Figure 7. Influences of the pressure; (a) influences of the pressureon the CHTC and (b) specific heat at constant pressure of the mixed working medium under different pressures

Kim [26] reveals that the specific heat at constant pressure at the boundary-layer of the flow substantially affects the CHTC when the fluid transfers heat at the supercritical conditions. The larger the specific heat at constant pressure is, the greater the CHTC. Figure 7(b) illustrates changes of the specific heat at constant pressure of the CO_2/R41 (51.4/48.6) mixture with the temperature under three different pressures. As shown, the specific heat at constant pressure always increases abruptly at the critical temperature. A comparison of figs 6 and 7 reveals that the CHTC changes in similar manner to the specific heat at constant pressure. This proves that even though the presence of the thread to some extent damages the

boundary-layer, the changes of the CHTC of the supercritical mixed working medium still match the results of Kim [26].

Furthermore, the CHTC of the working medium under three different pressures were compared. The result reveals that, with increasing pressure, the maximum CHTC of the working medium in the micro-fin tube decreases significantly, and the temperature corresponding to the maximum CHTC increases. The maximum CHTC under 7.0 MPa is twice that at 8.0 MPa. It is therefore inferred that the closer the heat transfer pressure to the critical pressure of the mixed working medium, the higher the maximum CHTC. In the case that the temperature is higher than the critical temperature, the heat transfer effect is better under high pressures.

Changes in the heat conductivity coefficient of the mixed working medium under different pressures with the temperature are shown in fig. 8. It is noteworthy that, although the specific heat under constant pressure, C_p, of the mixed working medium at non-critical temperatures is similar, the heat conductivity coefficient, λ, of the mixed working medium decreases with increasing temperature, fig. 8. In particular, the heat conductivity coefficient, λ, drops abruptly near the transcritical temperature. As a result, the heat conductivity coefficient of the mixed working medium under a low-temperature condition is larger than that under a high-temperature condition at a non-quasi-critical temperature.

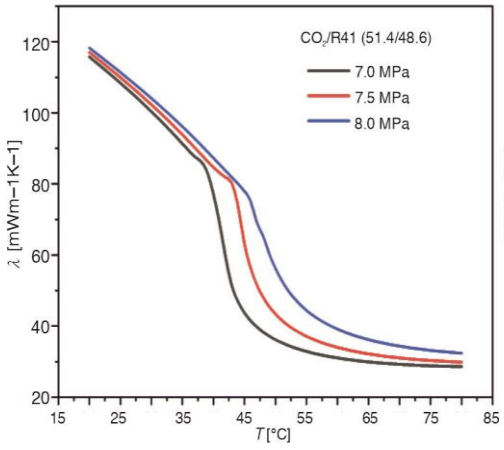

Figure 8. Heat conductivity coefficients of the mixed working medium under different pressures (*for color image see journal web site*)

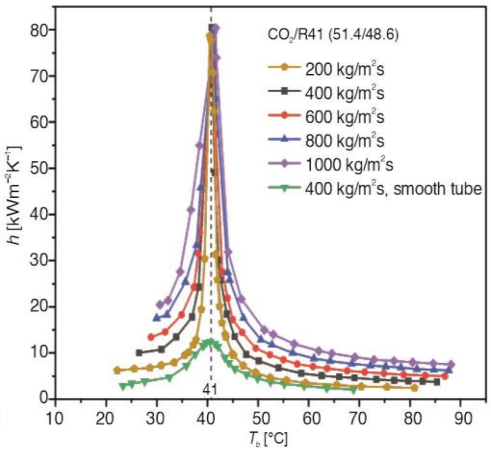

Figure 9. Influences of mass flux on the CHTC

By comparing the data obtained when using the micro-fin tube and smooth tube under 7.0 MPa in fig. 7, the following conclusions are reached:

- The temperature corresponding to the maximum CHTC is irrelevant to the structure of the heat-exchange tubes.
- The CHTC in the micro-fin tube is two to three times that of the smooth tube at a non-critical temperature.
- The difference in the heat transfer performance increases rapidly near the critical temperature, and the maximum CHTC in the micro-fin tube is as high as 80.5 kW/(m^2·K), while that in the smooth tube is only 12.4 kW/(m^2·K). The results show that the micro-fin tube significantly outperforms the smooth tube in terms of heat transfer.

Influences of mass flux

Figure 9 illustrates the CHTC of CO_2/R41 (51.4/48.6) under a pressure of 7.0 MPa at five mass fluxes 200, 400, 600, 800 and 1000 kg/m^{2}s, as well as changes of the CHTC of the fluid in the smooth tube at 400 kg/m^{2}s. The figure indicates that the maximum CHTC at 600 and 800 kg/m^{2}s are similar, and those at 200, 400, 1000 kg/m^{2}s are only slightly different from those under the other two mass fluxes. The result indicates that:

- The mass flux does not influence the temperature corresponding to the maximum CHTC, because the temperature corresponding to the maximum CHTC is mainly dependent on the specific heat at constant pressure, while the mass flux exerts no influences, as aforementioned.
- The mass flux exerts slight influences on the maximum CHTC of the mixed working medium.

By comparing performance of CO_2/R41 at a non-critical temperature under the three conditions in fig. 9, the higher the mass flux, the stronger the overall heat transfer performance in the micro-fin tube. At the non-critical temperature, the model at a mass flux of 800 kg/m^{2}s has a CHTC some 1.7 times that at 400 kg/m^{2}s. This is because, under turbulent flow conditions, a higher mass flux induces a higher turbulence intensity, thereby generating a better heat transfer performance. Figure 10 shows changes of the turbulence energy, *k*. in the micro-fin tube at the five mass fluxes, in which the turbulence energy at 800 kg/m^{2}s is about three times that at 400 kg/m^{2}s.

As for the upper limit of flow velocity, Webb [27] experimentally discovered (as early as in 1999) that, with the increase of the flow velocity of a working medium, the increase of CHTC first accelerates, then gradually slows. Subsequently, through research on micro-fin tubes, Zhang *et al.* [28] found that the growth rate of the CHTC attributed to mass flux decreases when the mass flux reaches 500 kg/m^{2}s. Such a non-linear phenomenon results from the complex interaction between the micro-fins and the fluid, including the liquid displacement due to surface tension and interfacial turbulence. The experimental data, fig. 10, show that the CHTC at the non-critical temperature improves by at least 1.4 kW/m^{2}K for each increase of 200 kg/m^{2}s in the mass flux. This means that the rate of change of the CHTC does not decrease as the mass flux increases from 600 to 800 or even 1000 kg/m^{2}s, which is probably attributable to the absence of a phase change in the new supercritical mixed working medium CO_2/R41.

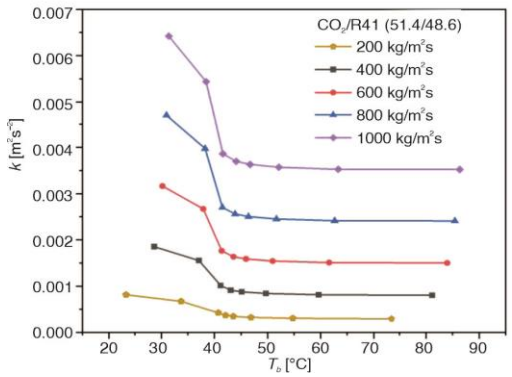

Figure 10. Influences of mass flux on the turbulence energy

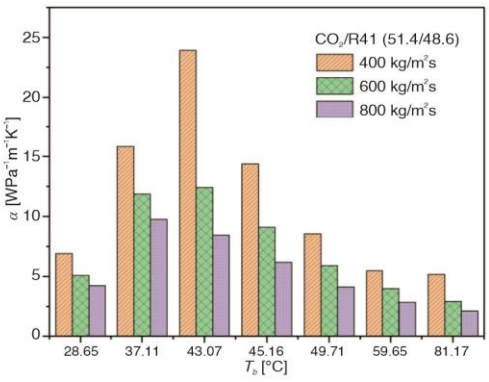

Figure 11. Influences of the mass flux on the heat transfer coefficient per unit pressure drop

The heat transfer enhancement by replacing the smooth tube with the micro-fin tube is realised at the cost of hydraulic performance, so the heat transfer performance and the hydraulic performance need to be traded off. In general, three methods can be used to evaluate the heat transfer enhancement: enhanced heat transfer under constant pump power, enhanced heat transfer at the same flow, and the comprehensive heat transfer under a constant pressure drop. The first is largely affected by the system and experiment and fails to characterise common phenomena with due precision, and its strongly systematic nature does not tally with the simulation of local heat exchange tubes. The second finds it difficult to describe the energy loss intuitively, therefore, the third method is used for comparison based on the heat transfer coefficient per unit pressure drop α.

As shown in fig. 11, with the increase of the mass flux, the heat transfer coefficient per unit pressure drop constantly declines: the value at 400 kg/m^{2}s is 1.5 to 3 times that at 800 kg/m^{2}s. When T_b is 316.22 K, the model, at a mass flux of 400 kg/m^{2}s has a heat transfer coefficient per unit pressure drop as high as 23.93 W/Pa·mK, while α in the model of a flow at 800 kg/m^{2}s is only 8.44 W/Pa·mK. The results suggest that the high mass flux more significantly increases the energy loss when remarkably enhancing the heat transfer performance, that is, the comprehensive thermo-hydraulic performance is poorer at a high mass flux rate.

It can be learnt that the condition of a higher mass flux can be selected if pursuing the extreme heat transfer performance, such as 800 kg/m^{2}s. Whereas, a low mass flux (400 kg/m^{2}s for instance) is suggested when comprehensively considering the energy consumption-output ratio. Moreover, maintaining the mixed working medium in a temperature range of 30 ℃ to 50 ℃ can ensure both an outstanding heat transfer performance and high overall performance.

Influences of components of the mixed working medium

If the CO_2 fraction is too high in the mixed working medium, the critical pressure is improved, for example, the critical pressure of CO_2/R41 (75/25) mixture is as high as 7.08 MPa. Therefore, a working condition with a pressure of 7.5 MPa was used to replace those at 7.0 MPa showing the optimal heat transfer performance above, to ensure all working media can normally enter the supercritical state. The mass flux was thus set to 400 kg/m^{2}s.

Figure 12 shows the changes of the CHTC of the mixed working media of three different components under the previous conditions with the bulk temperature. When other conditions remain unchanged, the higher the content of CO_2 is, the lower the temperature at the maximum CHTC and the higher the maximum CHTC. Therein, CO_2/R41 (75/25) exhibits the maximum CHTC as high as 77.42 kW/m^{2}K, while CO_2/R41 (20.5/79.5) has a maximum CHTC of 30.19 kW/m^{2}K. At temperatures greater than the critical value, the working medium containing a larger R41 fraction exhibits better heat transfer performance. Therein, the CHTC of CO_2/R41 (20.5/79.5) gradually stabilises at about 4.8 kW/m^{2}K, while that of CO_2/R41 (75/25) stabilises at around 3.4 kW/m^{2}K.

Figure 13 illustrates influences of components on the heat transfer coefficient per unit pressure drop. Near the quasi-critical temperature, the working medium containing a higher CO_2 fraction shows superiority in terms of its heat transfer performance, which is attributed to the excellent gas-like flow properties of CO_2, which can significantly reduce flow loss. For example, the maximum heat transfer coefficients per unit pressure drop of both CO_2/R41 (75/25) and CO_2/R41 (51.4/48.6) are greater than 25 W/Pa·mk, while that of CO_2/R41 (20.5/79.5) with a low CO_2 fraction is only 14.54 W/Pa·mk. The three do not exhibit any apparent difference at non-quasi-critical temperatures.

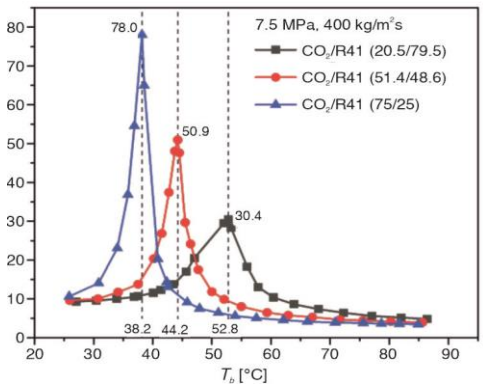

Figure 12. Influences of components on the CHTC

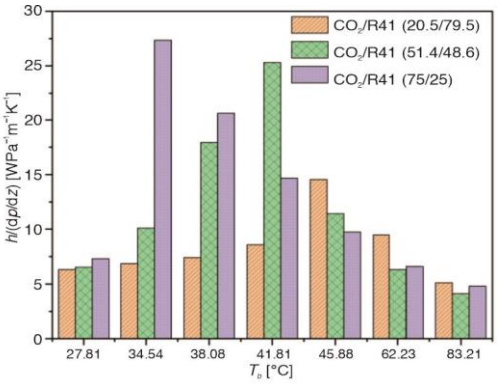

Figure 13. Influences of components on the heat transfer coefficient per unit pressure drop

Both the CHTC and the heat transfer coefficient per unit pressure drop increase under conditions when the CO_2 fraction is large. Despite this, as mentioned in Section 1, pure supercritical CO_2 has a large critical pressure and results in a very low COP of systems, which influences the actual range of application and other materials should be added for adjustment. Figure 14 shows the critical pressures corresponding to the CO_2/R41 mixtures with different CO_2 fractions. Taken together, when selecting mixtures of different components as the working media from the perspective of comprehensive evaluation, the mixture containing a higher CO_2 fraction is preferred if the working temperature is between 30 ℃ and 50 ℃. If the working temperature is beyond 30 ℃ to 50 ℃, the comprehensive evaluation of mixed working media of different components returns slightly different results, and the mixture containing a high R41 fraction can be selected to reduce the working pressure and improve the COP.

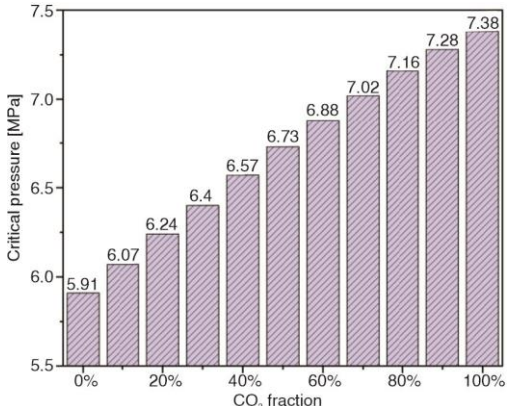

Figure 14. Critical pressures corresponding to the working media containing different CO_2 fractions

Conclusions

A model for 3-D analysis of a 5 mm micro-fin tube was established and validated. On this basis, the CO_2/R41 mixture was taken as the working medium to simulate its flow and heat transfer under the heat flux of 24 kW/m^2 and different pressures, mass fluxes, and components. By analysing the simulation results, the following conclusions are drawn:

- The CHTC increases abruptly near the critical temperature and is maximised at temperatures slightly above the critical temperature. It can be as high as 80.5 kW/mK, which is eight times higher compared with that at a non-critical temperature.
- The pressure influences the CHTC by affecting the specific heat of the working medium: the larger the pressure, the lower the maximum CHTC and the higher the temperature corresponding to the maximum CHTC. The maximum CHTC under 7.0 MPa is twice that under 8.0 MPa.

- The mass flux affects the CHTC by influencing the turbulence intensity: the larger the mass flux, the higher the overall CHTC, the lower the heat transfer coefficient per unit pressure drop, and the poorer the evaluation of the performance and energy consumption.
- The working medium containing a larger CO_2 fraction shows a higher CHTC and heat transfer coefficient per unit pressure drop at the critical temperature. For the working medium of a higher R41 fraction, its CHTC changes more slowly and its CHTC is higher at most working temperatures.

Acknowledgment

The authors gratefully acknowledge the support of National Natural Science Foundation of China (Grant No. 61871200) and Natural Science Foundation of Fujian province, China (Grant No. 2021J10854).

Nomenclature

C_p – specific heat at constant pressure, [kJkg^{-1}K^{-1}]
D – external diameter, [mm]
F – volume force vector, [Nm^{-3}]
G – mass flux, [kgm^{-2}s^{-1}]
h – convective heat transfer coefficient, [kWm^{-2}K^{-1}]
H_f – tooth depth, [mm]
I – vector of impulse, [kgms^{-2}]
k – turbulence energy, [m^{2}s^{-2}]
N – number of teeth, [–]
q – heat flux, [kWm^{-2}]
Q – total heat flux, [Wm^{-2}]
T_w – wall thickness, [mm]
T – temperature, [°C]
T_b – bulk temperature, [°C]
T_c – critical temperature [°C]
T_{in} – inlet temperature [°C]
T_{out} – outlet temperature [°C]
T_{wall} – wall temperature [°C]
u – velocity vector [ms^{-1}]
x – distance to the inlet [m]

Greek symbols

α – heat transfer coefficient per unit pressure drop [WPa^{-1}m^{-1}K^{-1}]
β – helical angle [°]
ε – dissipation rate [–]
λ – heat conductivity coefficient [mWm^{-1}K^{-1}]
μ – viscosity [Pa·s]
μ_T – eddy viscosity [Pa·s]
σ – turbulent Prandtl number [–]

References

[1] Lorentzen G., The Use of Natural Refrigerants: A Complete Solution to the CFC/HCFC Predicament, *International Journal of Refrigeration, 18* (1995), 3, pp. 190-197
[2] Oh, H., Son, C., New Correlation to Predict the Heat Transfer Coefficient In-Tube Cooling of Supercritical CO_2 in Horizontal Macro-Tubes, *Experimental Thermal and Fluid Science, 34* (2010), 8, pp. 1230-1241
[3] Pioro, I., Current Status of Research on Heat Transfer in Forced Convection of Fluids at Supercritical Pressures, *Nuclear Engineering and Design, 354* (2019), Dec.,110207
[4] Qwa, B., *et al*., The Three-Regime-Model for Pseudo-Boiling in Supercritical Pressure, *International Journal of Heat and Mass Transfer, 181* (2021), 121875
[5] Barghi, F., *et al*., Effect of Initial Wetting State on Plastron Recovery Through Heating, *International Journal of Heat and Mass Transfer, 156* (2020), 119705
[6] Kim, D., Kim, M., Experimental investigation of Heat Transfer in Vertical Upward and Downward Supercritical CO_2 Flow in a Circular Tube, *International Journal of Heat and Fluid Flow, 32* (2011), 1, pp. 176-191
[7] Peng, R., *et al*., Forced Convective Heat Transfer of Supercritical Carbon Dioxide in Mini-Channel Under Low Mass Fluxes, *International Journal of Heat and Mass Transfer, 182* (2022), 121919
[8] Zhang, X., *et al*., Determination of the Optimum Heat Rejection Pressure in Transcritical Cycles Working With R744/R290 Mixture, *Applied Thermal Engineering, 54* (2013), 1, pp. 176-184
[9] Onaka, Y., *et al*. Experimental study on Evaporation Heat Transfer of CO_2/DME Mixture Refrigerant in a Horizontal Smooth Tube, *International Journal of Refrigeration, 33* (2010), 7, pp. 1277-1291

[10] Sarkar, J., Bhattacharyya, S., Assessment of blends of CO_2 with butane and isobutane as Working Fluids for Heat Pump Applications, *International Journal of Thermal Sciences, 48* (2009), 7, pp. 1460-1465
[11] Ali, *et al*., Applying Refrigerant Mixtures with Thermal Glide in Cold Climate Air-Source Heat Pumps, *Applied Thermal Engineering, 62* (2014), 2, pp. 714-722
[12] Kim, J., *et al*., Cooling performance of several CO_2/Propane Mixtures and Glide Matching with Secondary Heat Transfer Fluid, *International Journal of Refrigeration, 31* (2008), 5, pp. 800-806
[13] Kim, J., *et al*., Circulation concentration of CO_2/Propane Mixtures and the Effect of their Charge on the Cooling Performance in an Air-Conditioning System, *International Journal of Refrigeration, 30* (2007), 1, pp. 43-49
[14] Dai B., *et al*., Thermodynamic Performance Assessment of Carbon Dioxide Blends with Low-Global Warming Potential (GWP) Working Fluids for a Heat Pump Water Heater, *International Journal of Refrigeration, 56* (2015), 1, pp. 1-14
[15] Wang, D., *et al*., Thermodynamic Analysis of CO_2 Blends with R41 as an Azeotropy Refrigerant Applied in Small Refrigerated Cabinet and Heat Pump Water Heater, *Applied Thermal Engineering, 125* (2017), Oct., pp. 1490-1500
[16] Yu, B., *et al*., Experimental Energetic Analysis of CO_2/R41 Blends in Automobile Air-Conditioning and Heat Pump Systems, *Applied Energy, 239* (2019), Apr., pp. 1142-1153
[17] Gradziel S., *et al*., Experimental Determination of the Heat Transfer Coefficient is Internally Rifled Tubes, *Thermal Science, 23* (2019), Suppl. 4, pp. S1163-S1174
[18] Lin, Y., *et al*., Numerical Investigation on Thermal Performance and Flow Characteristics OFZ and S Shape PCHE Using S-CO_2, *Thermal Science, 23* (2019), Suppl. 3, pp. S757-S764
[19] Cavallini, A., *et al*., Heat Transfer and Pressure Drop During Condensation of Refrigerants Inside Horizontal Enhanced Tubes, *International Journal of Refrigeration, 23* (2000), 1, pp. 4-25
[20] Cho, J., Kim, M., Experimental Studies on the Evaporative Heat Transfer and Pressure Drop of CO_2 in Smooth and Micro-Fin Tubes of the Diameters of 5 and 9.52 mm, *International Journal of Refrigeration, 30* (2007), 6, pp. 986-994
[21] Al-Fahed, S., *et al*., Pressure Drop and Heat Transfer Comparison for Both Micro-Fin Tube and Twisted-Tape Inserts in Laminar Flow, *Experimental Thermal and Fluid Science, 18* (1998), 4, pp. 323-333
[22] Kim, N., Evaporation Heat Transfer and Pressure Drop of R-410A in a 5.0 mm O.D. Smooth and Micro-Fin Tube, *International Journal of Air-Conditioning and Refrigeration, 23*(2015), 1, 1550004
[23] Ding, Y., Liu, J., Condensation Heat Transfer of R404A in Horizontal Inner-Threaded Tubes (in Chinese), *Journal of Engineering for Thermal Energy and Power, 32* (2020), 12, pp. 141-147
[24] Moosaie, A., *et al*., An Algebraic Closure Model for the DNS of Turbulent Drag Reduction by Brownian Microfiber Additives in a Channel Flow, *Journal of Non-Newtonian Fluid Mechanics., 226* (2015), Dec., pp. 60-66
[25] Xie, G, *et al*., Heat Transfer Behaviors of Some Supercritical Fluids: A Review, *Chinese Journal of Aeronautics, 35* (2022), 1, pp. 290-306
[26] Kim, D., Kim, M., Two Layers Heat Transfer Model for Supercritical Fluid Flow in a Vertical Tube, *The Journal of Supercritical Fluids, 58* (2011), 1, pp. 15-25
[27] Webb, R., *Heat Transfer Enhancement of Heat Exchangers, Prediction of Condensation and Evaporation in Micro-Fin and Micro-Channel Tubes*, Springer, Dordrecht, The Netherlands, 1999
[28] Zhang, J., *et al*., Numerical Simulation of R410A Condensation in Horizontal Micro-Fin Tubes, Numerical Heat Transfer Part A Application, *An International Journal of Computation and Methodology, 71* (2017), 4, pp. 361-376

Paper submitted: March 11, 2022
Paper revised: May 13, 2022
Paper accepted: May 14, 2022